Polarizable force field for CO_2 in M-MOF-74 derived from quantum mechanics

Becker, Tim M.; Lin, Li Chiang; Dubbeldam, David; Vlugt, Thijs J.H.

DOI
10.1021/acs.jpcc.8b08639

Publication date
2018

Document Version
Final published version

Published in
Journal of Physical Chemistry C

THE JOURNAL OF PHYSICAL CHEMISTRY C

Article

Cite This: J. Phys. Chem. C 2018, 122, 24488−24498

pubs.acs.org/JPCC

Polarizable Force Field for CO_2 in M-MOF-74 Derived from Quantum Mechanics

Tim M. Becker,[†] Li-Chiang Lin,[‡] David Dubbeldam,[†,§] and Thijs J. H. Vlugt*[,†]

[†]Engineering Thermodynamics, Process & Energy Department, Faculty of Mechanical, Maritime and Materials Engineering, Delft University of Technology, Leeghwaterstraat 39, 2628CB Delft, The Netherlands

[‡]William G. Lowrie Department of Chemical and Biomolecular Engineering, The Ohio State University, 151 W. Woodruff Avenue, Columbus, Ohio 43210, United States

[§]Van't Hoff Institute for Molecular Sciences, University of Amsterdam, Science Park 904, 1098XH Amsterdam, The Netherlands

Supporting Information

ABSTRACT: On the short term, carbon capture is a viable solution to reduce human-induced CO_2 emissions, which requires an energy efficient separation of CO_2. Metal−organic frameworks (MOFs) may offer opportunities for carbon capture and other industrially relevant separations. Especially, MOFs with embedded open metal sites have been shown to be promising. Molecular simulation is a useful tool to predict the performance of MOFs even before the synthesis of the material. This reduces the experimental effort, and the selection process of the most suitable MOF for a particular application can be accelerated. To describe the interactions between open metal sites and guest molecules in molecular simulation is challenging. Polarizable force fields have potential to improve the description of such specific interactions. Previously, we tested the applicability of polarizable force fields for CO_2 in M-MOF-74 by verifying the ability to reproduce experimental measurements. Here, we develop a predictive polarizable force field for CO_2 in M-MOF-74 (M = Co, Fe, Mg, Mn, Ni, Zn) without the requirement of experimental data. The force field is derived from energies predicted from quantum mechanics. The procedure is easily transferable to other MOFs. To incorporate explicit polarization, the induced dipole method is applied between the framework and the guest molecule. Atomic polarizabilities are assigned according to the literature. Only the Lennard-Jones parameters of the open metal sites are parameterized to reproduce energies from quantum mechanics. The created polarizable force field for CO_2 in M-MOF-74 can describe the adsorption well and even better than that in our previous work.

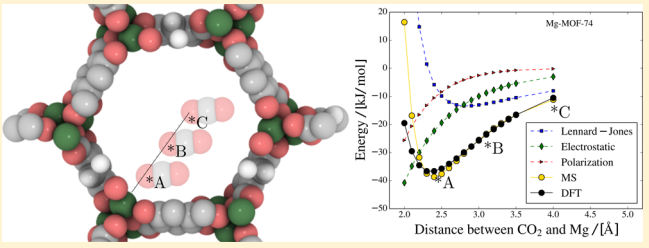

INTRODUCTION

Anthropogenic CO_2 emissions correlate strongly with climate change.[1] To mitigate the consequences of burning fossil fuels, carbon capture has been proposed.[2,3] In carbon capture, the CO_2 emitted (e.g., from power plants) is separated from the flue gas instead of being released into the atmosphere. The physical adsorption of gas molecules in metal−organic frameworks (MOFs) has potential for practical realization of this separation,[1,4] as well as, for the separation of oxygen, hydrogen, and gaseous hydrocarbons.[5] It is important to note that it is not a trivial task to select the best or even a suitable MOF for a given separation.[6] Theoretically, MOFs can be built with a huge variety of structures and chemical compositions.[7,8] The synthesis of a multitude of MOFs and adsorption experiments can be cumbersome and expensive.[9] Molecular simulation (MS) offers a possibility to predict adsorption properties before conducting lab experiments.[10] Thereby, MS enables the computational preselection of promising MOFs.[9,11,12] Subsequently, lab experiments can focus on these promising structures. In particular, MOFs featuring open metal sites have been shown to selectively adsorb some constituents of gases.[13] Hence, these MOFs are of special interest for a variety of applications such as the separation of hydrocarbons[14,15] and carbon capture.[16] The large selectivity is a result of strong interactions between some guest molecules and the open metal sites.[17] MS is based on force fields which describe the interactions between the different molecules considered. The quality of the predictions depends on how well these interactions are modeled.[18] The enhanced interactions between guest molecules and open metal sites were partially ascribed to polarization of the guest molecules located close to the open metal sites.[19−26] Until now, explicit polarization is rarely considered in Monte Carlo simulations of MOFs.[18,20,27,28] Not considering polarization in a heterogeneous electrostatic environment has been pointed out as an explanation why many generic force fields fail to describe the correct adsorption in MOFs.[18,20,28] A polarizable force field which is applicable to a large variety of MOFs is therefore of great interest to guide the selection process for gas separations via solid adsorbents.[29] Besides, the improved understanding

Received: September 4, 2018
Revised: October 8, 2018
Published: October 9, 2018

and design of the electrostatic environment could be beneficial to better customize MOFs for certain applications.[30] Unfortunately, excessive computational costs do still prevent polarizable force fields from being widely applied in Monte Carlo simulations.[27] In our previous work, we verified the potential of polarizable force field for CO_2 in M-MOF-74 by adjusting the force field to reproduce experimental measurements.[27,32] The applied method is based on induced dipoles and has also been successfully applied to model xylenes in NaY zeolite by Lachet et al.[31] The advantage of the method is the rapid computational time which is comparable to the time when polarization is not considered. In this study, a polarizable force field for CO_2 in M-MOF-74 (M = Co, Fe, Mg, Mn, Ni, Zn) is developed directly from quantum mechanics (QM). Compared with our previous work, this procedure is predictive and no prior experiments are necessary. This is of particular interest for hypothetical MOFs[8] that have not been synthesized and no experimental data are available. Adjustments are made to the Lennard-Jones (LJ) force field parameters of the metal atoms which act as open metal sites. These sites are considered to interact strongly with the guest molecules.[33] The new parameters are determined by reproducing energies computed from density functional theory (DFT) calculations. DFT energies for different positions of a CO_2 molecule on paths toward the interaction sites of the framework are taken from Mercado et al.[34] and Lee et al.[35] For Mn-MOF-74, the DFT energies were directly provided by Dr. Kyuho Lee. The details regarding these calculations are analogous to his published work.[35] Similar procedures have been successfully conducted for nonpolarizable force fields.[33,34,36] Polarization is added to simplify the development of the force field by introducing a model with better physical justification and reducing the number of adjustable variables. Additional parameters to describe the polarizability of interaction sites are assigned according to the literature and are not considered adjustable. Simultaneously, explicit polarization might improve the transferability of the resulting force field. The more physical model can potentially lead to a better understanding of the true adsorption.

The detailed procedure on how the polarizable force field is developed from QM is presented in the Methodology section. To investigate the predictive potential of the approach, adsorption isotherms and heats of adsorptions for CO_2 in M-MOF-74 with six different metal atoms, that is, Co, Fe, Mg, Mn, Ni, and Zn, are calculated. Subsequently, computational results are compared with experimental results.[16,37−39] In comparison to a nonpolarizable force field, this approach has the potential to require less adjustable parameters by considering environments with different polarity directly.[21,28,30] Moreover, the computational time is comparable to standard Monte Carlo simulations without explicit polarization. We believe that the development of polarizable force fields is a step toward a more realistic description of MOFs and simultaneously to more transferable force fields.

METHODOLOGY

The development of force fields from QM for MOFs has been the focus of many recent scientific studies.[23,40−44] In general, the procedure is based on predicting the potential energy surface from, for example, DFT or MP2 and to subsequently optimize the force field parameters in such a way that the potential energy surface is well reproduced. If the force field can describe the correct potential energy surface, it is anticipated to reliably model the adsorption because locations of single guest molecules and interactions strengths are presumably described well. Of course, assumptions such as the rigidity of the framework and entropic effects may introduce uncertainties. In general, the accuracy of the potential energy surface is determined by the chosen QM method[34,44,45] and the number of relevant points on the potential energy surface used to describe it. A trade-off between accuracy and computational time has to be made.[44] Different levels of theory, the amount and type of basis sets, and the size of the considered system can affect computational time and accuracy. Here, we chose DFT energies as reference that were carefully validated by Lee et al.[35] For the classical force field, it is of particular importance to model the most favorable adsorption sites well because these sites are dictating the adsorption. As mentioned previously, several studies have been investigating the derivation of force fields from QM to describe adsorption in MOFs.[23,33,34,36,40,41,43,46] In these studies, Monte Carlo simulations were applied which rarely considered explicit polarizable force fields, even though polarizable force fields have the potential to improve performance and transferability.[19−21,25] Motivated by the failure of generic force fields, McDaniel et al.[47] developed a predictive polarizable force field for CO_2[47,48] and CH_4[18] in several ZIFs and other MOFs. These authors modeled polarization of guest molecules via the shell model[49] while neglecting explicit polarization of the framework. In addition to introducing solely polarization, the interactions between framework and guest molecules were re-parameterized with a nonstandard functional form. Good agreement between experiments and computational results was achieved. The overhead in computational time introduced by polarization slowed the conducted Monte Carlo simulations down by a factor of 2−10 in comparison to standard simulations. Furthermore, substantial work concerning polarizable force fields for MOFs with open metal sites has been carried out by the group of Space et al. Initially, the group focused on adsorption of H_2 in MOFs with open metal sites.[19−21,25,28] Recently, these authors also developed force fields for CO_2[30,50,51] and even small hydrocarbons.[51] To consider polarization, the induced dipole method was applied. The computational results were accurate and showed that considering polarization is crucial for describing the correct adsorption of MOFs with open metal sites. The computational costs of considering explicit polarization in Monte Carlo simulations, however, was as high as 95% of the total computational time. In this study, likewise Monte Carlo simulations are conducted. Explicit polarization is added to the force field via the induced dipole method.[49,52] Back-polarization is neglected to achieve reasonable simulation times that are in the same order as force fields without considering explicit polarization. The required dipole polarizabilities α_i are taken from the literature without being adjusted.[53,54] The resulting induction energy U_{ind} can be determined from[31]

$$U_{ind} = -\frac{1}{2}\sum_{i=1}^{n} \alpha_i \cdot |E_i^0|^2 \quad (1)$$

where E_i^0 is the electric field created by the framework at interaction site i of the moved guest molecule which consists of n sites. More simulation details can be found in our previous studies[27,32] and the work of Lachet et al.[31] Here, LJ force field parameters of nonmetal atoms for M-MOF-74 are assigned

DOI: 10.1021/acs.jpcc.8b08639
J. Phys. Chem. C 2018, 122, 24488−24498

according to the UFF force field,[55] a generic force field frequently used for the modeling of MOFs.[21,25,30,48] For CO_2, the TraPPE force field is applied which is commonly used to describe CO_2 adsorbed in MOFs.[56] The TraPPE force field describes the vapor−liquid equilibrium of CO_2 well.[56] Polarization is exclusively considered between the framework and guest molecules. Interactions between guest molecules are calculated according to the TraPPE force field. The LJ force field parameters of the metal sites are adjusted to reproduce the potential energy surface previously predicted from QM. These metal sites interact particularly strongly with guest molecules and are known to be inadequately modeled by generic force fields.[19,20,44] The DFT energies describing the potential energy surface are computed for CO_2 configurations on paths toward atom sites of the MOF frameworks. As an example, Figure 1 provides an overview of the varying atom sites of Mg-MOF-74.

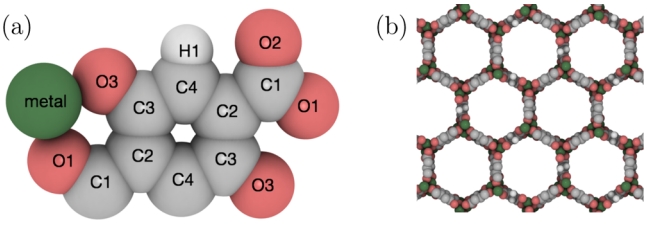

Figure 1. (a) Schematic view of the varying atom sites and (b) the framework of Mg-MOF-74. Magnesium, carbon, oxygen, and hydrogen are depicted in green, gray, red, and white, respectively.[57]

The other M-MOF-74 frameworks are represented analogously. For every M-MOF-74 framework, nine different atom types can be identified to describe the local environment: the corresponding metal atoms, three different oxygens O1, O2, O3, four different carbons, C1, C2, C3, C4, and hydrogen, H1. Energy paths are considered toward all atom types besides hydrogen, as in the work of Mercado et al.[34] and Lin et al.[36] A grid search is conducted to determined LJ force field parameters of the metal atoms. ϵ values and σ values are evaluated ranging from 5.0 to 140.0 K and from 2.4 to 3.3 Å, respectively. For every grid point, the energies predicted from DFT are compared with energies calculated with a polarizable force field for all CO_2 configurations on all energy paths. The objective function used to evaluate the modeling of the total energy on the energy paths toward the various interaction sites is

$$\min\left(\sum_{j}^{\text{all paths}} \exp\left[\frac{-E_j^{\text{DFT}}}{k_B \cdot T}\right] \cdot |E_j^{\text{DFT}} - E_j^{\text{MS}}|\right) \quad (2)$$

E_j^{DFT} and E_j^{MS} are energies determined via DFT or molecular simulation, respectively, for a CO_2 configuration j on one of the energy paths. k_B is the Boltzmann constant and T the temperature of the conducted MS (i.e., 298 K). The Boltzmann weight is applied to consider differences in energy and to prioritize more relevant configurations which are lower in energy.[44] The presented approach is straightforward and easy to apply. The aim is to create a predictive polarizable force field that describes the potential energy surface well and can be evaluated with an efficiency comparable to nonpolarizable force fields. The effect of polarization is implicitly included in the DFT energies and should be modeled approximately by matching the energies of all energy paths simultaneously while using the induced dipole method in MS with point polarizabilities taken from literature. Polarizable force fields have the potential to provide improved transferability by considering environments with various polarities.[19−21]

SIMULATION DETAILS

Grand-canonical Monte Carlo simulations as implemented in the RASPA software package[58,59] are conducted to compute the uptake and heat of adsorption of CO_2 in different structures of M-MOF-74 (M = Co, Fe, Mg, Mn, Ni, Zn). The pure component uptakes are computed for varying fugacities at 298 K up to 10 bar. MOF structures with atomic charges are taken from previous studies.[34−36] The Ewald summation technique with a relative precision of 10^{-6} is used to calculate electrostatic interactions between static point charges.[10] All frameworks are considered to be rigid. The LJ potential is truncated at a cutoff distance of 12 Å without being shifted and without analytic tail corrections. To mimic a continuous system, periodic boundary conditions are applied. Multiple unit cells are chosen to represent the simulated system and to ensure a minimum distance of more than twice the cutoff radius between periodic images. LJ force field parameters for CO_2 are taken from the TraPPE force field.[56] Interactions between CO_2 molecules are not modified and computed based on the original force field. For nonmetal atoms of M-MOF-74, LJ force field parameters of the UFF force field are assigned.[55] Cross-interactions are calculated via the Lorentz−Berthelot mixing rules from atomic parameters.[60] Explicit polarization is considered via the induced dipole method (cf. eq 1).[31] Polarization is exclusively considered between the framework and guest molecules. Back-polarization is neglected. The required atomic polarizabilties α_i are taken from Applequist et al.[53] Details on the final force field parameters are listed in the Supporting Information. For the comparison of simulation results with available experimental measurements reported in the literature, the Peng−Robinson equation of state is used to convert pressures to fugacities.[61]

RESULTS AND DISCUSSION

An overview of the results of the grid search is shown in Figure 2 exemplary for Ni-MOF-74.

To present the result clearly, the final value of the objective function is scaled between 0 and 1, where 0 represents the lowest and 1 represents the highest value. The objective function is the sum of the difference in total energy between DFT and MS weighted by the Boltzmann factor (cf. eq 2). The results of the objective function show that a range of force field parameters for the metal site starting at the upper left corner of Figure 2 and continuing to the lower right corner provides similar agreement between DFT and MS energies. The results reveal a common problem of force field fitting, namely, that the force field parameters are often not unambiguous. The lowest value of the objective function can be observed for ϵ of 32.5 K and σ of 2.8 Å for the metal site. The results of the grid search corresponding to the other investigated M-MOF-74 structures illustrate very similar trends and can be found in the Supporting Information. The best found force field parameters together with the value of the corresponding objective function relative to the sum of the objective function for all M-MOF-74 frameworks are summarized in Table 1.

DOI: 10.1021/acs.jpcc.8b08639
J. Phys. Chem. C 2018, 122, 24488−24498

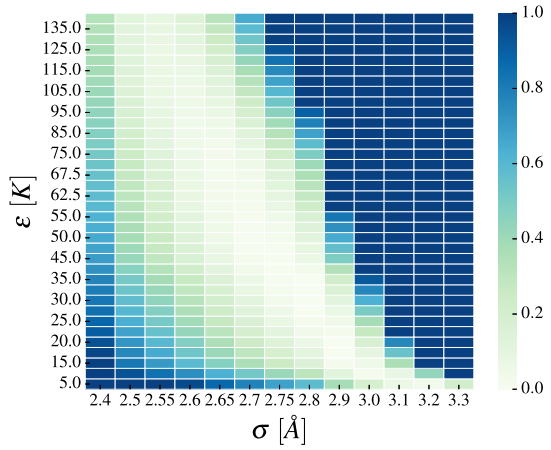

Figure 2. Graphic representation of the outcome of the grid search for ϵ and σ of the metal site of Ni-MOF-74. The shown values represent the results of the objective function scaled between 0 and 1. The lowest value of the objective function is represented by 0 while the largest value corresponds to 1.

Table 1. Optimal LJ Force Field Parameters for the Metal Sites Determined via the Grid Search[a]

structure	ϵ [K]	σ [Å]	objective function [%]
Co-MOF-74	30.0	2.75	0.7
Fe-MOF-74	5.0	3.2	0.9
Mg-MOF-74	5.0	3.0	78.7
Mn-MOF-74	5.0	3.1	17.2
Ni-MOF-74	32.5	2.8	2.1
Zn-MOF-74	70.0	2.9	0.4

[a]Value of the objective function relative to the sum of objective functions for all frameworks.

The parameters for Fe, Mg, and Mn lie on the edge of the parameter space considered in the grid search. However, we observed that enlarging the search range of the grid does not improve the objective function significantly. For this study, we decided to continue with the chosen grid which contains a reasonable parameter space. For Mn-MOF-74 and particularly for Mg-MOF-74, the relative values of the objective function are large. Consequently, the description of the CO_2 energy paths for these frameworks seems to be relatively poor in comparison to the other frameworks. In this context, Figure 3 compares the DFT energy paths toward all metal sites.

The comparison reveals that the DFT energy path for the Mg site is around 10 kJ/mol lower in energy than for the other metals, whereas the paths for the Co-, Fe-, Mn-, and Ni-based frameworks have a similar lowest energy. This results in a larger value for the objective function of Mg-MOF-74 because the difference in energy is weighted with the Boltzmann factor at 298 K. However, the actual quality of the description of the DFT energy paths for Mg-MOF-74 and the other frameworks is comparable. The case of Mn-MOF-74 is more complicated. The minimum of the Mn energy path is located closer to the framework than for the other metals with similar minimum energy (cf. Figure 3). The large value of the objective function may be a result of the location of the minimum because the DFT energy paths toward the nonmetal interaction sites are comparable for all frameworks. Overall, the chosen objective function suggests that the energy paths are less well modeled for Mn-MOF-74 than for the other frameworks. In Figure 4, all energy paths for CO_2 toward the various interaction sites of

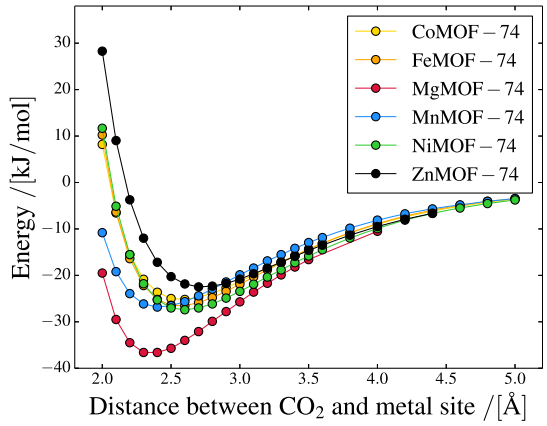

Figure 3. DFT energy paths towards the open metal sites for all investigated M-MOF-74 frameworks.

Mn-MOF-74 are compared between the developed polarizable force field and DFT results.

It is obvious that the agreement between the DFT energy paths and the paths obtained with the developed polarizable force field is not perfect. As a result of the grid search, we observed that the Mn and the O1 energy paths cannot be accurately reproduced concurrently. This is important because both paths are low in energy and therefore crucial for the correct description (cf. Figure 4a,b). Interestingly, Mercado et al.[34] also experienced difficulties when modeling the adsorption of CO_2 in Mn-MOF-74. These authors did not report a force field for this framework. Besides the comparison between DFT and MS energies, the underlying energy contributions to the total energy predicted with the polarizable force field are shown. These contributions are polarization energy, electrostatic energy, and LJ energy (dispersion and repulsion). A similar energy decomposition is very difficult to achieve in DFT calculations for periodic systems and it is not possible for most available QM packages. In the case of Mn-MOF-74, static electrostatic and polarization energies are contributing considerably to the total energy of the Mn and O1 paths but are less relevant for the other paths. This is expected as the CO_2 molecule is supposed to be polarized in the vicinity of the open metal site.[30] Especially, the repulsive region cannot be reproduced accurately by the polarizable force field. The difficulty to model this region could be caused by LJ repulsion. Because of overall strong interactions, the energy minima of the energy paths are located close to the framework. At these short distances, the LJ contribution of the energy increases too rapidly and dominates the total energy. For example, in case of the optimal position of the CO_2 molecule on the path toward the open metal site, the LJ potential is already in the repulsive region (cf. Figure 4a). In addition, static electrostatics and polarization contribute considerably. As a result, a fragile balance between the different energy contributions is created when the binding distance is particularly short. The LJ potential was designed rather for computational convenience and especially the repulsive part is nonphysical[44] and normally assumed to be modeled poorly.[23,51] This can lead to inaccuracies in the description, especially for systems with very short binding distances as in the case of MOFs with open metal sites. Another functional form, like in the Buckingham potential which requires an additional fitting parameter, might be closer to reality and therefore more reasonable to describe the repulsion.[41] Finally, it would be beneficial to develop a

DOI: 10.1021/acs.jpcc.8b08639
J. Phys. Chem. C 2018, 122, 24488−24498

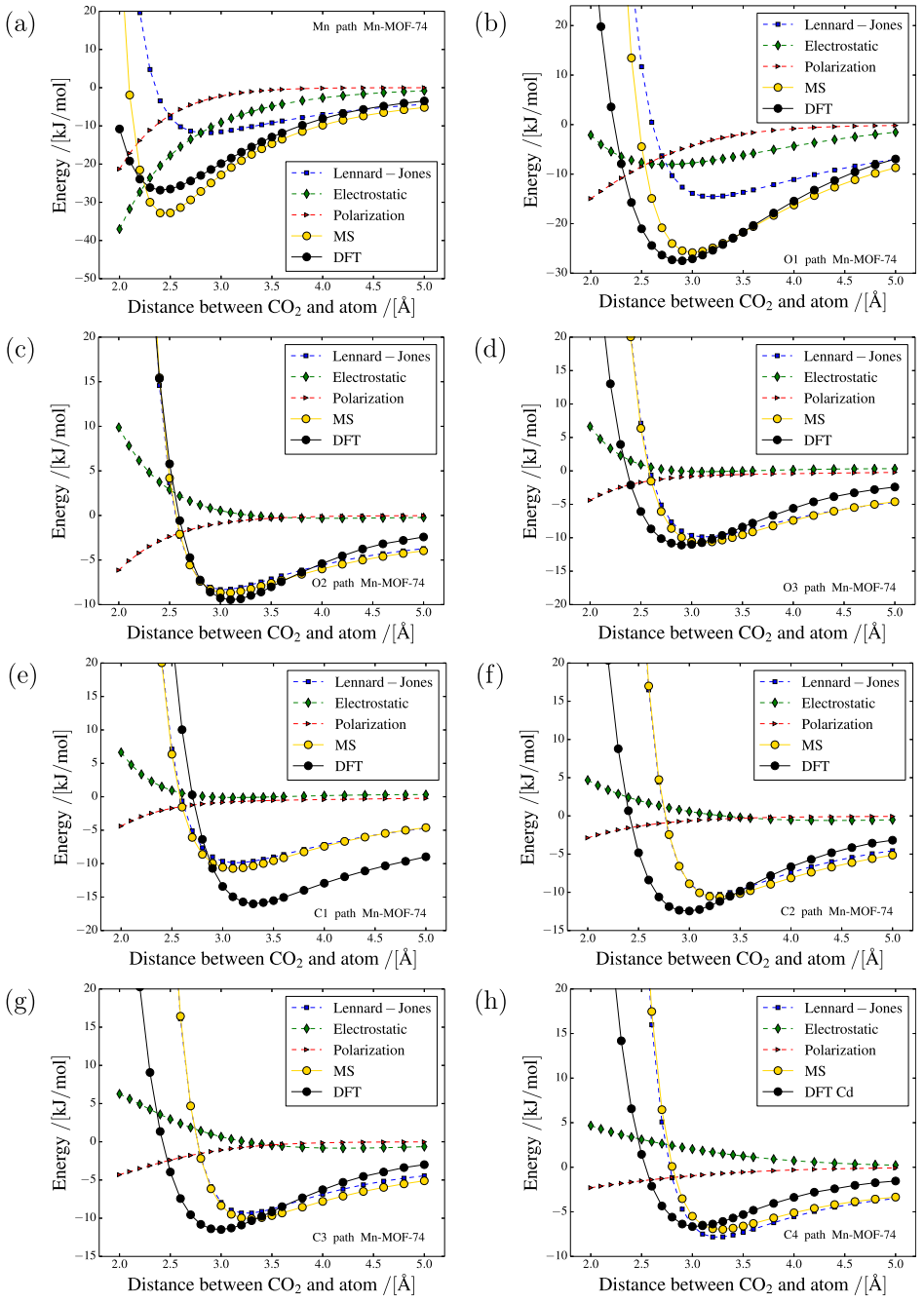

Figure 4. Comparison of energy paths towards (a) Mn, (b) O1, (c) O2, (d) O3, (e) C1, (f) C2, (g) C3, and (h) C4 for Mn-MOF-74 determined via DFT and MS with the polarizable force field. Additionally, the different contributions of the MS energy are shown: LJ, static electrostatics, and polarization.

completely new polarizable force field without any parameters from previous generic force fields.[62−65] Then, the balance between the underlying energy contributions could be improved for short binding distances. The energy paths for the other M-MOF-74 frameworks which agree better between DFT and MS are provided in the Supporting Information. Figure 5 provides an overview of the adsorption isotherms predicted with the developed polarizable force field for all considered M-MOF-74 frameworks and compares the computational results to computational[34] and experimental[16,37−39] measurements from various other studies.

Overall, the newly designed polarizable force field agrees well with the experimental measurements. Different shapes of the adsorption isotherms can be reproduced by only adjusting the LJ parameters of the metal sites. The agreement is slightly worse than that of the nonpolarizable force field of Mercado et al.[34] Somewhat larger deviations can be observed for Co-MOF-74, and Ni-MOF-74. However, to develop their force field, Mercado et al.[34] adjusted not only the LJ parameters of the metal site but all interaction sites. Thereby, the approach of these authors has more fitting parameters and the potential energy surface can be eventually described better. At the same time, the approach is much more elaborate and the resulting force field parameters might be less transferable. In contrast to this study, these authors additionally scaled all adsorption isotherms by a constant factor of 0.85 to account for structural

DOI: 10.1021/acs.jpcc.8b08639
J. Phys. Chem. C 2018, 122, 24488−24498

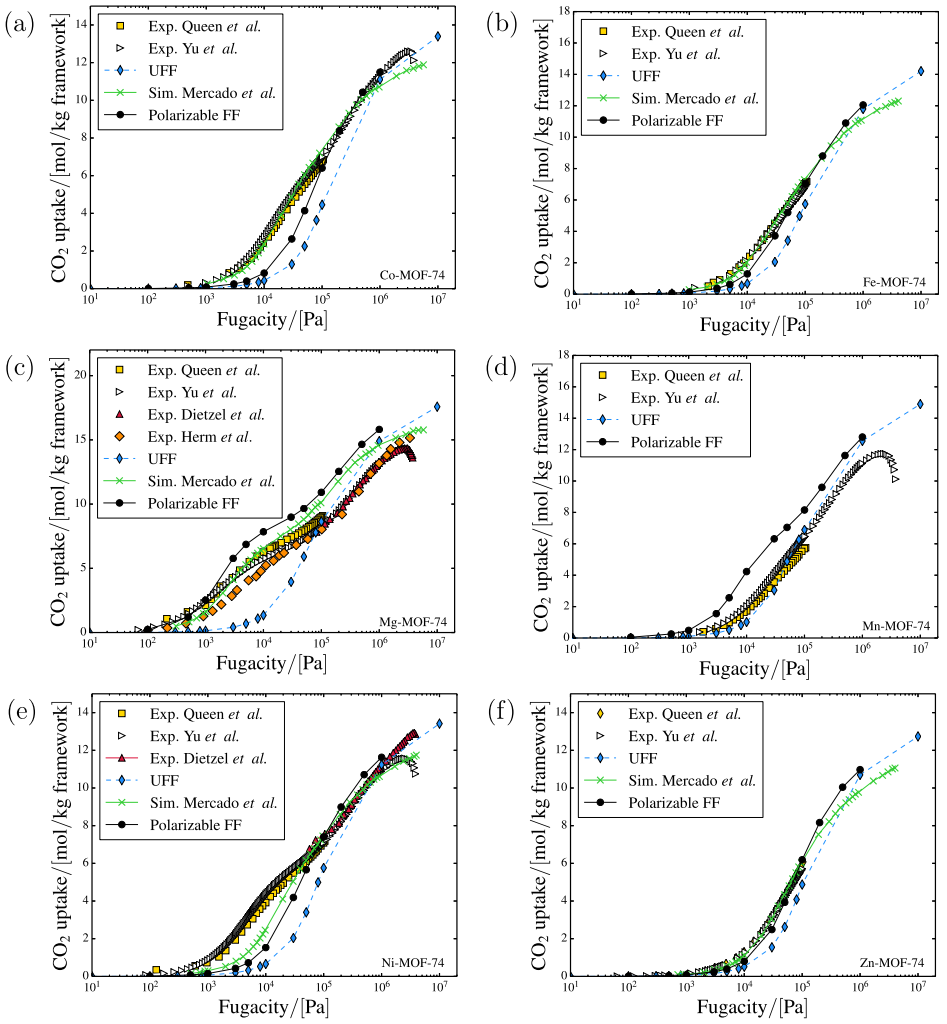

Figure 5. Adsorption isotherms for CO_2 in (a) Co-MOF-74, (b) Fe-MOF-74, (c) Mg-MOF-74, (d) Mn-MOF-74, (e) Ni-MOF-74, and (f) Zn-MOF-74 at 298 K. Comparison between the developed polarizable force field, the computational results of Mercado et al.,[34] simulations performed with the UFF force field,[66] and experimental measurement of various studies.[16,37−39]

defects. Hence, we are satisfied with the obtained degree of agreement. The computational predictions using the UFF force field cannot describe the experimental data. The adsorption isotherms for frameworks with varying metal ions are predicted to be similar. The larger deviations between experiments and simulations in the adsorption isotherms of Mn-MOF-74 in comparison to the other frameworks might be a consequence of the poor agreement of the energy paths for this framework. As mentioned previously, Mercado et al.[34] did not publish a force field for Mn-MOF-74. These authors reported that they could not reproduce the adsorption isotherm even though they could reproduce the varying energy paths well. The poor agreement could potentially originate from many possible reasons, for example, the used atomic structures, the point charge model, or uncertainties in the DFT calculations. To investigate the precise reason is very challenging and beyond the scope of this study. The corresponding comparison of heats of adsorptions for all investigated frameworks is shown in Figure 6.

The computational results are compared with heats of adsorptions that are derived from experimental adsorption isotherms via the Clausius−Clapeyron equation[67] by different studies.[16,38,39] This method can be sensitive to the specific experimental input.[50] However, in the absence of measurements it is the usual benchmark. The computed heats of adsorption follow the trends predicted with the Clausius−Clapeyron equation. The developed polarizable model is able to model the heat of adsorption as a function of the CO_2 uptake. While the overall agreement is good, larger deviations can be observed for the Co, Mn, and Ni-based frameworks. These are the same frameworks that showed deviations for the adsorption isotherms. If the frequently used UFF force field is assigned to the metal sites, the distinct differences between the varying frameworks cannot be modeled. Although the adsorption is already relatively well modeled by the developed polarizable model, there is further improvement possible. For Mg-MOF-74 and Mn-MOF-74, the final LJ energy parameters are on the lower boarder of the considered grid. Close to the minimum of the total energy of the metal path, the total energy almost exclusively consists of static electrostatic and polarization energy. Hence, LJ parameters are favored that contribute only slightly to the total energy of the metal path. As a result, the LJ contribution of the metal site to the other energy paths should be small, as well. To further improve the agreement, we have also explored the possibility to include the charges assigned to the framework atoms as fitting parameters in the grid search via a simple scaling. Framework charges are often considered as one of the simulation inputs. However,

DOI: 10.1021/acs.jpcc.8b08639
J. Phys. Chem. C 2018, 122, 24488−24498

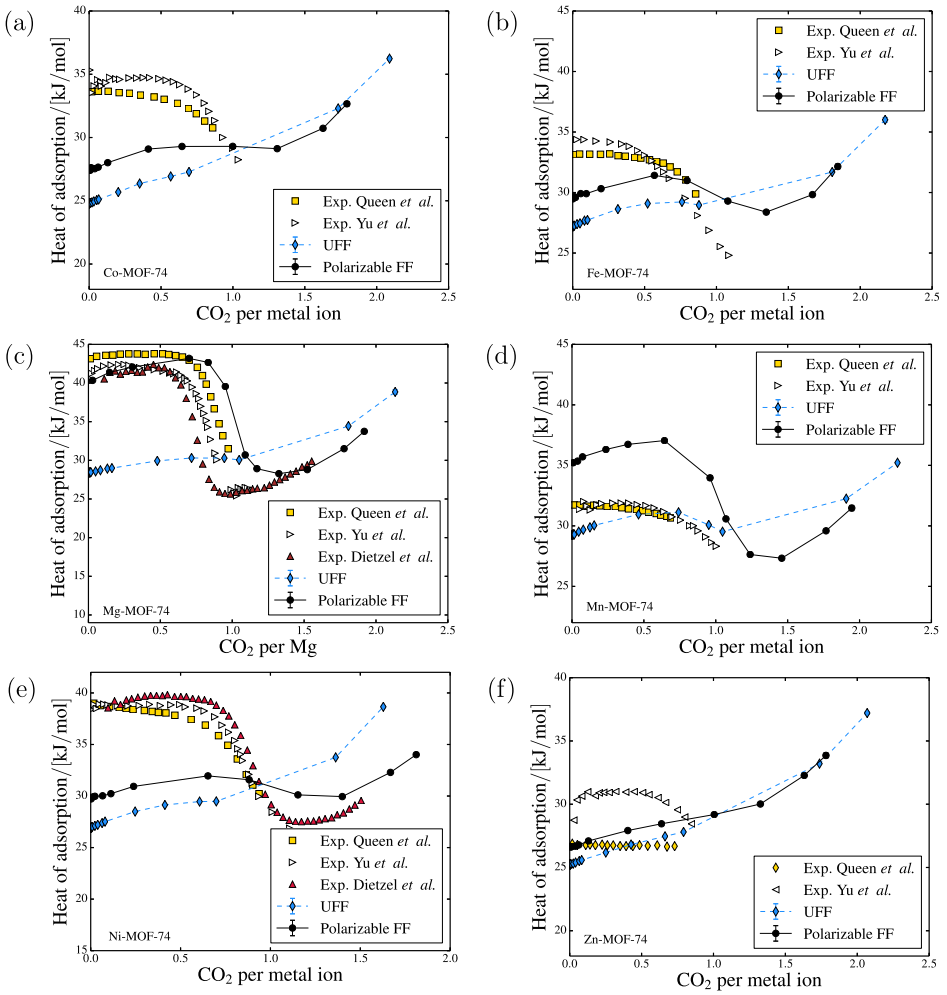

Figure 6. Heats of adsorption for CO_2 in (a) Co-MOF-74, (b) Fe-MOF-74, (c) Mg-MOF-74, (d) Mn-MOF-74, (e) Ni-MOF-74, and (f) Zn-MOF-74 at 298 K. Comparison between the developed polarizable force field, simulations performed with the UFF force field[66] and results obtained via the Clausius−Clapeyron equation of various studies.[16,38,39]

many different procedures exist to actually fit point charges to the individual interaction sites.[68] Unfortunately, a large sensitivity can be observed for some systems. By reducing the framework charges, the contributions of both the static electrostatic energy and the polarization energy are lowered. The main objective of scaling the point charges is to investigate if the differently determined LJ parameters positively influence the overall agreement between DFT and MS paths, especially, for the paths that are less influenced by static electrostatic and polarization energy. Consequently, we conducted an additional grid search for Mg-MOF-74 and Mn-MOF-74 in which the point charges and the LJ parameters are varied. Here, all framework charges are scaled with a constant factor f ($q_i^{new} = q_i^{old} \cdot f$). We conducted the grid search for f values of 0.95, 0.925, 0.9, 0.85, 0.8, 0.75, and 0.7. The final outcome of this grid search including charge scaling is summarized in Table 2.

For both frameworks, the best agreement between DFT and MS energy paths could be achieved for a uniform point charge reduction of 10%. In case of Mn-MOF-74, all energy paths improved. However, the improvement of the objective function relative toward the objective function without charge scaling of Mn-MOF-74 is only 10%. Hence, the modeling of the energy paths for Mn-MOF-74 is still less accurate than for the other frameworks (cf. Table 1). For Mg-MOF-74, the value of the objective function improved by a factor of 5. The

Table 2. Final LJ Force Field Parameters Determined via the Grid Search with Charge Scaling[a]

structure	ε [K]	σ [Å]	f	relative improvement [%]
Mg-MOF-74	5.0	2.8	0.9	0.196
Mn-MOF-74	105.0	2.4	0.9	0.909

[a]The improvement is measured relative to the previous individual objective function without charge scaling.

improvement results from a better description of the Mg paths. A slight improvement of this path causes a huge change in the objective function because it is substantially lower in energy than the other energy paths. The other energy paths for Mg-MOF-74 remain approximately the same or in the case of O1 even worsen. All related energy paths with scaled charges for Mg-MOF-74 and Mn-MOF-74 can be found in the Supporting Information. The corresponding adsorption isotherms are shown in Figure 7.

The predicted adsorption isotherm for Mg-MOF-74 changes mainly in the low-pressure region. Because of the changed parameters, the adsorption isotherm moves closer to the one predicted by Mercado et al.[34] Both adsorption isotherms seem to be acceptable. The one with scaled and the one without scaled charges are in the range of experimental measurements and the change is rather small. As expected by the rather small

DOI: 10.1021/acs.jpcc.8b08639
J. Phys. Chem. C 2018, 122, 24488−24498

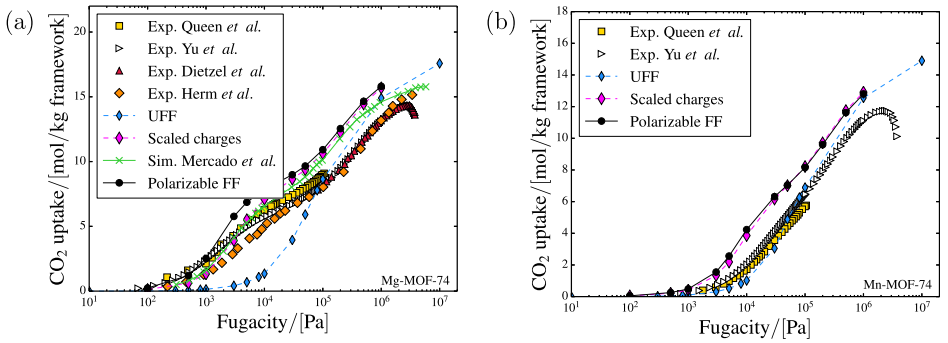

Figure 7. Adsorption isotherms for CO_2 with and without charge scaling in (a) Mg-MOF-74 and (b) Mn-MOF-74 at 298 K. Comparison between the developed polarizable force field, the computational results of Mercado et al.,[34] simulations performed with the UFF force field,[66] and experimental measurement of various studies.[16,37−39]

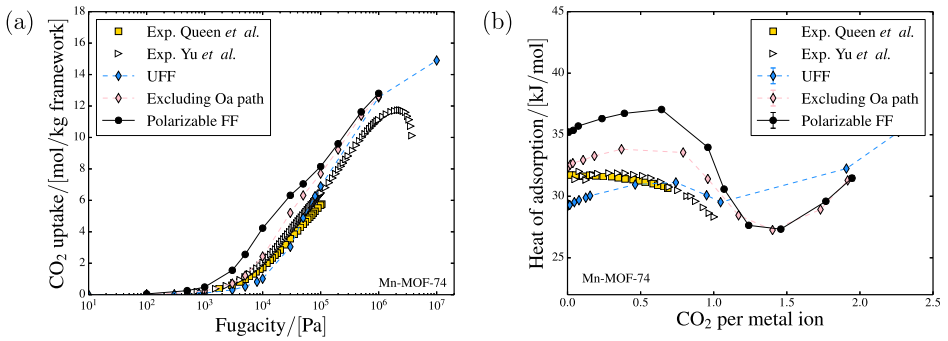

Figure 8. (a) Adsorption isotherms and (b) heat of adsorption for CO_2 in Mn-MOF-74 at 298 K with and without considering the O1 energy path in the grid search. Comparison between the developed polarizable force field, the computational results of Mercado et al.,[34] simulations performed with the UFF force field,[66] and experimental measurement of various studies.[38,39]

improvement in the objective function, the adsorption isotherm for Mn-MOF-74 changes slightly. Still, the agreement between the experimental and predicted adsorption isotherms for Mn-MOF-74 is rather poor. In a related work, Lin et al.[36] suggested to not consider the energy paths of the O1 site for the development of a H_2O force field because the O1 site is located further away from the surface of M-MOF-74. Following this idea, we excluded the energy path for O1 in the evaluation of the grid search for Mn-MOF-74. The best parameters excluding the O1 energy paths for the Mn-based framework are f = 0.9, ϵ = 5.0 K, and σ = 3.0 Å. The corresponding energy paths can be found in the Supporting Information. As expected, the energy path toward the O1 site is less well reproduced than when considering it in the evaluation of the grid search. The description of the Mn energy path is improved even though the repulsion part is still not well reproduced. The computed adsorption isotherm and heat of adsorption predicted with the new parameter set are presented in Figure 8.

Apparently, the modeling of the adsorption is improved both for the adsorption isotherm as well as for the heat of adsorption. A possible reason may be the improvement in the description of the minimum in the Mn energy path. As mentioned previously, the minimum energy is located closer to the metal site than for the other frameworks with comparable minimum energy. At this distance, the total energy depends strongly on the repulsion in the LJ potential of the Mn site. Unfortunately, an improvement caused by the deletion of the O1 energy path in the evaluation of the grid search cannot be observed for the remaining frameworks. Instead, for the other frameworks, the opposite behavior can be observed; the agreement between experimental measurements and computational predictions becomes poorer. This is intuitive because the energy paths are merely points on the potential energy surface which should in general be described better if more points are considered in the fitting. As suggested by Mercado et al.,[34] the underlying issue to describe Mn-MOF-74 might be more complicated and further investigations are needed.

CONCLUSIONS

The presented procedure to derive polarizable force fields is fully predictive. To consider explicit polarization, the induced dipole method was applied. Because of previously introduced simplifications, the computational time is similar to standard Monte Carlo simulations without considering explicit polarization. The used atomic polarizabilities were taken from the literature without further adjustment. No prior experimental data are required for the development. A grid search has been conducted to adjust the LJ parameters of the open metal sites. The results confirm that the procedure works well and that the experimentally measured adsorption is reproduced. Besides, the procedure is relatively simple and easily transferable to other MOFs with open metal sites. By the explicit consideration of polarization in MS, the contribution of polarization is physically interpretable and can provide further knowledge of the underlying mechanisms of the molecular system. This might help to customize MOFs that perform even better for certain applications. Tuning the electrostatic environment could potentially be very useful. The comparison between DFT and MS energy paths reveals that differences arise mainly in the repulsive region of the LJ potential. Typically, this region is badly described by a LJ potential. In

DOI: 10.1021/acs.jpcc.8b08639
J. Phys. Chem. C 2018, 122, 24488−24498

the case of MOFs with open metal sites, it is of more importance than usually because the guest molecules interact strongly with the open metal sites and binding distances are short. Further improvement can be expected when improving the modeling of the repulsive region of the potential. This might be achieved by a more realistic functional form such as the Buckingham potential. For M-MOF-74, significant effects of static electrostatic interactions and polarization can be observed for the paths toward the open metal sites and toward the O1 site. The contribution of electrostatics is less for the energy paths toward the other interaction sites. Uniformly adjusting the framework charges together with the LJ parameters of the metal sites showed relatively small effects for Mg-MOF-74 and Mn-MOF-74. In contrast, not considering the energy path toward the O1 site could improve the description of the experimentally observed adsorption for Mn-MOF-74. However, for the remaining frameworks, the inclusion of the O1 energy path was beneficial. Ultimately, the complete set of force field parameters should be consistently deducted from QM. A predictive, transferable, and polarizable force field created in such a fashion would be of great value. Such a potential has the potential to improve the understanding of the adsorption but also to computationally screen MOFs for specific applications.

■ ASSOCIATED CONTENT

Supporting Information

The Supporting Information is available free of charge on the ACS Publications website at DOI: 10.1021/acs.jpcc.8b08639.

Tables containing force field parameters of the developed polarizable force field; figures giving an overview of the grid search; and the energy paths for all presented force field parameters (PDF)

■ AUTHOR INFORMATION

Corresponding Author

*E-mail: t.j.h.vlugt@tudelft.nl.

ORCID

Tim M. Becker: 0000-0002-6601-4320
Li-Chiang Lin: 0000-0002-2821-9501
David Dubbeldam: 0000-0002-4382-1509
Thijs J. H. Vlugt: 0000-0003-3059-8712

Notes

The authors declare no competing financial interest.

■ ACKNOWLEDGMENTS

This work was sponsored by NWO Exacte Wetenschappen (Physical Sciences) for the use of supercomputer facilities, with the financial support from the Nederlandse Organisatie voor Wetenschappelijk Onderzoek (Netherlands Organization for Scientific Research, NWO). T.J.H.V. acknowledges NWO-CW (Chemical Sciences) for a VICI grant. The authors also thank the Ohio Supercomputer Center (OSC)[69] for the computational resources. We would like to acknowledge Dr. Kyuho Lee for sharing the DFT-computed reference energies in Mn-MOF-74.

■ REFERENCES

(1) Smit, B.; Reimer, J. R.; Oldenburg, C. M.; Bourg, I. C. *Introduction to Carbon Capture and Sequestration*, 1st ed.; Imperial College Press: London, 2014; Vol. *1*.

(2) Chu, S. Carbon Capture and Sequestration. *Science* **2009**, *325*, 1599.

(3) Sumida, K.; Rogow, D. L.; Mason, J. A.; McDonald, T. M.; Bloch, E. D.; Herm, Z. R.; Bae, T.-H.; Long, J. R. Carbon Dioxide Capture in Metal-Organic Frameworks. *Chem. Rev.* **2012**, *112*, 724−781.

(4) Huck, J. M.; Lin, L.-C.; Berger, A. H.; Shahrak, M. N.; Martin, R. L.; Bhown, A. S.; Haranczyk, M.; Reuter, K.; Smit, B. Evaluating Different Classes of Porous Materials for Carbon Capture. *Energy Environ. Sci.* **2014**, *7*, 4132−4146.

(5) Li, J.-R.; Sculley, J.; Zhou, H.-C. Metal-Organic Frameworks for Separations. *Chem. Rev.* **2012**, *112*, 869−932.

(6) Colón, Y. J.; Fairen-Jimenez, D.; Wilmer, C. E.; Snurr, R. Q. High-Throughput Screening of Porous Crystalline Materials for Hydrogen Storage Capacity near Room Temperature. *J. Phys. Chem. C* **2014**, *118*, 5383−5389.

(7) Rowsell, J. L. C.; Yaghi, O. M. Metal-Organic Frameworks: A New Class of Porous Materials. *Microporous Mesoporous Mater.* **2004**, *73*, 3−14.

(8) Wilmer, C. E.; Leaf, M.; Lee, C. Y.; Farha, O. K.; Hauser, B. G.; Hupp, J. T.; Snurr, R. Q. Large-Scale Screening of Hypothetical Metal-Organic Frameworks. *Nat. Chem.* **2012**, *4*, 83−89.

(9) Lin, L.-C.; Berger, A. H.; Martin, R. L.; Kim, J.; Swisher, J. A.; Jariwala, K.; Rycroft, C. H.; Bhown, A. S.; Deem, M. W.; Haranczyk, M.; Smit, B. In Silico Screening of Carbon-Capture Materials. *Nat. Mater.* **2012**, *11*, 633−641.

(10) Frenkel, D.; Smit, B. *Understanding Molecular Simulation*, 2nd ed.; Academic Press: San Diego, 2002.

(11) Kim, J.; Lin, L.-C.; Martin, R. L.; Swisher, J. A.; Haranczyk, M.; Smit, B. Large-Scale Computational Screening of Zeolites for Ethane/Ethene Separation. *Langmuir* **2012**, *28*, 11914−11919.

(12) Erdős, M.; de Lange, M. F.; Kapteijn, F.; Moultos, O. A.; Vlugt, T. J. H. In Silico Screening of Metal-Organic Frameworks for Adsorption-Driven Heat Pumps and Chillers. *ACS Appl. Mater. Interfaces* **2018**, *10*, 27074−27087.

(13) Dietzel, P. D. C.; Panella, B.; Hirscher, M.; Blom, R.; Fjellvåg, H. Hydrogen Adsorption in a Nickel based Coordination Polymer with Open Metal Sites in the Cylindrical Cavities of the Desolvated Framework. *Chem. Commun.* **2006**, 959−961.

(14) Bae, Y.-S.; Lee, C. Y.; Kim, K. C.; Farha, O. K.; Nickias, P.; Hupp, J. T.; Nguyen, S. T.; Snurr, R. Q. High Propene/Propane Selectivity in Isostructural Metal-Organic Frameworks with High Densities of Open Metal Sites. *Angew. Chem., Int. Ed.* **2012**, *51*, 1857−1860.

(15) Geier, S. J.; Mason, J. A.; Bloch, E. D.; Queen, W. L.; Hudson, M. R.; Brown, C. M.; Long, J. R. Selective Adsorption of Ethylene over Ethane and Propylene over Propane in the Metal-Organic Frameworks M_2(dobdc) (M = Mg, Mn, Fe, Co, Ni, Zn). *Chem. Sci.* **2013**, *4*, 2054−2061.

(16) Dietzel, P. D. C.; Besikiotis, V.; Blom, R. Application of Metal-Organic Frameworks with Coordinatively Unsaturated Metal Sites in Storage and Separation of Methane and Carbon Dioxide. *J. Mater. Chem.* **2009**, *19*, 7362−7370.

(17) Yazaydin, A. Ö.; Snurr, R. Q.; Park, T.-H.; Koh, K.; Liu, J.; LeVan, M. D.; Benin, A. I.; Jakubczak, P.; Lanuza, M.; Galloway, D. B. Screening of Metal-Organic Frameworks for Carbon Dioxide Capture from Flue Gas Using a Combined Experimental and Modeling Approach. *J. Am. Chem. Soc.* **2009**, *131*, 18198−18199.

(18) McDaniel, J. G.; Li, S.; Tylianakis, E.; Snurr, R. Q.; Schmidt, J. R. Evaluation of Force Field Performance for High-Throughput Screening of Gas Uptake in Metal−Organic Frameworks. *J. Phys. Chem. C* **2015**, *119*, 3143−3152.

(19) Belof, J. L.; Stern, A. C.; Eddaoudi, M.; Space, B. On the Mechanism of Hydrogen Storage in a Metal-Organic Framework Material. *J. Am. Chem. Soc.* **2007**, *129*, 15202−15210.

(20) Belof, J. L.; Stern, A. C.; Space, B. An Accurate and Transferable Intermolecular Diatomic Hydrogen Potential for Condensed Phase Simulation. *J. Chem. Theory Comput.* **2008**, *4*, 1332−1337.

DOI: 10.1021/acs.jpcc.8b08639
J. Phys. Chem. C 2018, 122, 24488−24498

(21) Forrest, K. A.; Pham, T.; McLaughlin, K.; Belof, J. L.; Stern, A. C.; Zaworotko, M. J.; Space, B. Simulation of the Mechanism of Gas Sorption in a Metal-Organic Framework with Open Metal Sites: Molecular Hydrogen in PCN-61. *J. Phys. Chem. C* **2012**, *116*, 15538−15549.
(22) Gutiérrez-Sevillano, J. J.; Dubbeldam, D.; Rey, F.; Valencia, S.; Palomino, M.; Martín-Calvo, A.; Calero, S. Analysis of the ITQ-12 Zeolite Performance in Propane-Propylene Separations Using a Combination of Experiments and Molecular Simulations. *J. Phys. Chem. C* **2010**, *114*, 14907−14914.
(23) Haldoupis, E.; Borycz, J.; Shi, H.; Vogiatzis, K. D.; Bai, P.; Queen, W. L.; Gagliardi, L.; Siepmann, J. I. Ab Initio Derived Force Fields for Predicting CO_2Adsorption and Accessibility of Metal Sites in the Metal-Organic Frameworks M-MOF-74 (M = Mn, Co, Ni, Cu). *J. Phys. Chem. C* **2015**, *119*, 16058−16071.
(24) Dubbeldam, D.; Walton, K. S. In *Metal−Organic Frameworks: Materials Modeling towards Engineering Applications*, 1st ed.; Jiang, J., Ed.; CRC Press: Boca Raton, 2015; pp 53−112.
(25) Pham, T.; Forrest, K. A.; Hogan, A.; McLaughlin, K.; Belof, J. L.; Eckert, J.; Space, B. Simulations of Hydrogen Sorption in rht-MOF-1: Identifying the Binding Sites Through Explicit Polarization and Quantum Rotation Calculations. *J. Mater. Chem. A* **2014**, *2*, 2088−2100.
(26) Cirera, J.; Sung, J. C.; Howland, P. B.; Paesani, F. The Effects of Electronic Polarization on Water Adsorption in Metal-Organic Frameworks: H_2Oin MIL-53(Cr). *J. Chem. Phys.* **2012**, *137*, 054704.
(27) Becker, T. M.; Dubbeldam, D.; Lin, L.-C.; Vlugt, T. J. H. Investigating Polarization Effects of CO_2Adsorption in MgMOF-74. *J. Comput. Sci.* **2016**, *15*, 86−94.
(28) Pham, T.; Forrest, K. A.; Banerjee, R.; Orcajo, G.; Eckert, J.; Space, B. Understanding the H_2Sorption Trends in the M-MOF-74 Series (M = Mg, Ni, Co, Zn). *J. Phys. Chem. C* **2015**, *119*, 1078−1090.
(29) Morris, W.; Leung, B.; Furukawa, H.; Yaghi, O. K.; He, N.; Hayashi, H.; Houndonougbo, Y.; Asta, M.; Laird, B. B.; Yaghi, O. M. A Combined Experimental-Computational Investigation of Carbon Dioxide Capture in a Series of Isoreticular Zeolitic Imidazolate Frameworks. *J. Am. Chem. Soc.* **2010**, *132*, 11006−11008.
(30) Pham, T.; Forrest, K. A.; Gao, W.-Y.; Ma, S.; Space, B. Theoretical Insights into the Tuning of Metal Binding Sites of Paddlewheels in rht-Metal-Organic Frameworks. *ChemPhysChem* **2015**, *16*, 3170−3179.
(31) Lachet, V.; Boutin, A.; Tavitian, B.; Fuchs, A. H. Computational Study of p-Xylene/m-Xylene Mixtures Adsorbed in NaY Zeolite. *J. Phys. Chem. B* **1998**, *102*, 9224−9233.
(32) Becker, T. M.; Heinen, J.; Dubbeldam, D.; Lin, L.-C.; Vlugt, T. J. H. Polarizable Force Fields for $CO_2$and ACH_4dsorption in M-MOF-74. *J. Phys. Chem. C* **2017**, *121*, 4659−4673.
(33) Dzubak, A. L.; Lin, L.-C.; Kim, J.; Swisher, J. A.; Poloni, R.; Maximoff, S. N.; Smit, B.; Gagliardi, L. Ab Initio Carbon Capture in Open-Site Metal-Organic Frameworks. *Nat. Chem.* **2012**, *4*, 810−816.
(34) Mercado, R.; Vlaisavljevich, B.; Lin, L.-C.; Lee, K.; Lee, Y.; Mason, J. A.; Xiao, D. J.; Gonzalez, M. I.; Kapelewski, M. T.; Neaton, J. B.; et al. Force Field Development from Periodic Density Functional Theory Calculations for Gas Separation Applications Using Metal-Organic Frameworks. *J. Phys. Chem. C* **2016**, *120*, 12590−12604.
(35) Lee, K.; Howe, J. D.; Lin, L.-C.; Smit, B.; Neaton, J. B. Small-Molecule Adsorption in Open-Site Metal-Organic Frameworks: A Systematic Density Functional Theory Study for Rational Design. *Chem. Mater.* **2015**, *27*, 668−678.
(36) Lin, L.-C.; Lee, K.; Gagliardi, L.; Neaton, J. B.; Smit, B. Force-Field Development from Electronic Structure Calculations with Periodic Boundary Conditions: Applications to Gaseous Adsorption and Transport in Metal-Organic Frameworks. *J. Chem. Theory Comput.* **2014**, *10*, 1477−1488.
(37) Herm, Z. R.; Swisher, J. A.; Smit, B.; Krishna, R.; Long, J. R. Metal-Organic Frameworks as Adsorbents for Hydrogen Purification and Precombustion Carbon Dioxide Capture. *J. Am. Chem. Soc.* **2011**, *133*, 5664−5667.
(38) Yu, D.; Yazaydin, A. O.; Lane, J. R.; Dietzel, P. D. C.; Snurr, R. Q. A Combined Experimental and Quantum Chemical Study of CO_2Adsorption in the Metal-Organic Framework CPO-27 with Different Metals. *Chem. Sci.* **2013**, *4*, 3544−3556.
(39) Queen, W. L.; Hudson, M. R.; Bloch, E. D.; Mason, J. A.; Gonzalez, M. I.; Lee, J. S.; Gygi, D.; Howe, J. D.; Lee, K.; Darwish, T. A.; et al. Comprehensive Study of Carbon Dioxide Adsorption in the Metal-Organic Frameworks M_2(dobdc) (M = Mg, Mn, Fe, Co, Ni, Cu, Zn). *Chem. Sci.* **2014**, *5*, 4569−4581.
(40) Chen, L.; Grajciar, L.; Nachtigall, P.; Düren, T. Accurate Prediction of Methane Adsorption in a Metal-Organic Framework with Unsaturated Metal Sites by Direct Implementation of an Ab Initio Derived Potential Energy Surface in GCMC Simulation. *J. Phys. Chem. C* **2011**, *115*, 23074−23080.
(41) Chen, L.; Morrison, C. A.; Düren, T. Improving Predictions of Gas Adsorption in Metal-Organic Frameworks with Coordinatively Unsaturated Metal Sites: Model Potentials, Ab Initio Parameterization, and GCMC Simulations. *J. Phys. Chem. C* **2012**, *116*, 18899−18909.
(42) Fang, H.; Kamakoti, P.; Ravikovitch, P. I.; Aronson, M.; Paur, C.; Sholl, D. S. First Principles Derived, Transferable Force Fields for CO_2Adsorption in Na-Exchanged Cationic Zeolites. *Phys. Chem. Chem. Phys.* **2013**, *15*, 12882−12894.
(43) Borycz, J.; Lin, L.-C.; Bloch, E. D.; Kim, J.; Dzubak, A. L.; Maurice, R.; Semrouni, D.; Lee, K.; Smit, B.; Gagliardi, L. CO_2 Adsorption in Fe_2(dobdc): A Classical Force Field Parameterized from Quantum Mechanical Calculations. *J. Phys. Chem. C* **2014**, *118*, 12230−12240.
(44) Fang, H.; Demir, H.; Kamakoti, P.; Sholl, D. S. Recent Developments in First-Principles Force Fields for Molecules in Nanoporous Materials. *J. Mater. Chem. A* **2014**, *2*, 274−291.
(45) Poloni, R.; Smit, B.; Neaton, J. B. CO_2Capture by Metal-Organic Frameworks with van der Waals Density Functionals. *J. Phys. Chem. A* **2012**, *116*, 4957−4964.
(46) Fang, H.; Kamakoti, P.; Zang, J.; Cundy, S.; Paur, C.; Ravikovitch, P. I.; Sholl, D. S. Prediction of CO_2Adsorption Properties in Zeolites Using Force Fields Derived from Periodic Dispersion-Corrected DFT Calculations. *J. Phys. Chem. C* **2012**, *116*, 10692−10701.
(47) McDaniel, J. G.; Yu, K.; Schmidt, J. R. Ab Initio, Physically Motivated Force Fields for CO_2Adsorption in Zeolitic Imidazolate Frameworks. *J. Phys. Chem. C* **2012**, *116*, 1892−1903.
(48) McDaniel, J. G.; Schmidt, J. R. Robust, Transferable, and Physically Motivated Force Fields for Gas Adsorption in Functionalized Zeolitic Imidazolate Frameworks. *J. Phys. Chem. C* **2012**, *116*, 14031−14039.
(49) Rick, S. W.; Stuart, S. J. In *Reviews in Computational Chemistry*, 1st ed.; Lipkowitz, K. B., Boyd, D. B., Ed.; John Wiley & Sons, Inc.: Hoboken, 2003; Vol. *18*, pp 89−146.
(50) Pham, T.; Forrest, K. A.; Franz, D. M.; Guo, Z.; Chen, B.; Space, B. Predictive Models of Gas Sorption in a Metal-Organic Framework with Open-Metal Sites and Small Pore Sizes. *Phys. Chem. Chem. Phys.* **2017**, *19*, 18587−18602.
(51) Franz, D. M.; Dyott, Z. E.; Forrest, K. A.; Hogan, A.; Pham, T.; Space, B. Simulations of Hydrogen, Carbon Dioxide, and Small Hydrocarbon Sorption in a Nitrogen-Rich rht-Metal-Organic Framework. *Phys. Chem. Chem. Phys.* **2018**, *20*, 1761−1777.
(52) Antila, H. S.; Salonen, E. In *Biomolecular Simulations*, 1st ed.; Monticelli, L., Salonen, E., Eds.; Humana Press: Clifton, 2013; pp 215−241.
(53) Applequist, J.; Carl, J. R.; Fung, K.-K. Atom Dipole Interaction Model for Molecular Polarizability. Application to Polyatomic Molecules and Determination of Atom Polarizabilities. *J. Am. Chem. Soc.* **1972**, *94*, 2952−2960.
(54) Shannon, R. D. Dielectric Polarizabilities of Ions in Oxides and Fluorides. *J. Appl. Phys.* **1993**, *73*, 348−366.
(55) Rappe, A. K.; Casewit, C. J.; Colwell, K. S.; Goddard, W. A.; Skiff, W. M. UFF, a Full Periodic Table Force Field for Molecular

DOI: 10.1021/acs.jpcc.8b08639
J. Phys. Chem. C 2018, 122, 24488−24498

Mechanics and Molecular Dynamics Simulations. *J. Am. Chem. Soc.* **1992**, *114*, 10024−10035.
(56) Potoff, J. J.; Siepmann, J. I. Vapor-Liquid Equilibria of Mixtures Containing Alkanes, Carbon Dioxide, and Nitrogen. *AIChE J.* **2001**, *47*, 1676−1682.
(57) Dubbeldam, D.; Calero, S.; Vlugt, T. J. H. iRASPA: GPU-Accelerated Visualization Software for Materials Scientists. *Mol. Simul.* **2018**, *44*, 653−676.
(58) Dubbeldam, D.; Calero, S.; Ellis, D. E.; Snurr, R. Q. RASPA: Molecular Simulation Software for Adsorption and Diffusion in Flexible Nanoporous Materials. *Mol. Simul.* **2016**, *42*, 81−101.
(59) Dubbeldam, D.; Torres-Knoop, A.; Walton, K. S. On the Inner Workings of Monte Carlo Codes. *Mol. Simul.* **2013**, *39*, 1253−1292.
(60) Schnabel, T.; Vrabec, J.; Hasse, H. Unlike Lennard-Jones Parameters for Vapor-Liquid Equilibria. *J. Mol. Liq.* **2007**, *135*, 170−178.
(61) Peng, D.-Y.; Robinson, D. B. A New Two-Constant Equation of State. *Ind. Eng. Chem. Fundam.* **1976**, *15*, 59−64.
(62) Wang, J.; Cieplak, P.; Li, J.; Hou, T.; Luo, R.; Duan, Y. Development of Polarizable Models for Molecular Mechanical Calculations I: Parameterization of Atomic Polarizability. *J. Phys. Chem. B* **2011**, *115*, 3091−3099.
(63) Wang, J.; Cieplak, P.; Li, J.; Wang, J.; Cai, Q.; Hsieh, M. J.; Lei, H.; Luo, R.; Duan, Y. Development of Polarizable Models for Molecular Mechanical Calculations II: Induced Dipole Models Significantly Improve Accuracy of Intermolecular Interaction Energies. *J. Phys. Chem. B* **2011**, *115*, 3100−3111.
(64) Wang, J.; Cieplak, P.; Cai, Q.; Hsieh, M.-J.; Wang, J.; Duan, Y.; Luo, R. Development of Polarizable Models for Molecular Mechanical Calculations. 3. Polarizable Water Models Conforming to Thole Polarization Screening Schemes. *J. Phys. Chem. B* **2012**, *116*, 7999−8008.
(65) Wang, J.; Cieplak, P.; Li, J.; Cai, Q.; Hsieh, M.-J.; Luo, R.; Duan, Y. Development of Polarizable Models for Molecular Mechanical Calculations. 4. van der Waals Parametrization. *J. Phys. Chem. B* **2012**, *116*, 7088−7101.
(66) Rappe, A. K.; Goddard, W. A. Charge Equilibration for Molecular-Dynamics Simulations. *J. Phys. Chem.* **1991**, *95*, 3358−3363.
(67) Perry, R. H.; Green, D. W.; Maloney, J. O.; Abbott, M. M.; Ambler, C. M.; Amero, R. C. *Perry's Chemical Engineers' Handbook*; McGraw-Hill: New York, 1997; Vol. 7.
(68) Hamad, S.; Balestra, S. R. G.; Bueno-Perez, R.; Calero, S.; Ruiz-Salvador, A. R. Atomic Charges for Modeling Metal-Organic Frameworks: Why and How. *J. Solid State Chem.* **2015**, *223*, 144−151.
(69) Ohio Supercomputer Center. http://osc.edu/ark:/19495/f5s1ph73 (accessed October 15, 2018).

DOI: 10.1021/acs.jpcc.8b08639
J. Phys. Chem. C 2018, 122, 24488−24498